Time series analysis of the Caspian Sea shoreline in response to sea level fluctuation using remotely sensed data

Elahe Akbari, Saeid Hamzeh, Ataolah Abdolahi Kakroodi, Mohamed Maanan

Regional Studies in Marine Science

Available online 14 September 2022, 102672

Time series analysis of the Caspian Sea shoreline in response to sea level fluctuation using remotely sensed data

Elahe Akbari[a] Saeid Hamzeh[b] Ataolah Abdolahi Kakroodi[b] Mohamed Maanan[c]

[a] Department of Remote Sensing and GIS, Faculty of Geography and Environmental sciences, Hakim Sabzevari University, Sabzevar, Iran

[b] Department of Remote Sensing and GIS, Faculty of Geography, University of Tehran, Tehran, Iran

[c] Université de Nantes, LETG UMR CNRS 6554, B.P. 81223, 44312, Nantes Cedex 3, France

Received 10 February 2021, Revised 30 August 2022, Accepted 10 September 2022, Available online 14 September 2022.

https://doi.org/10.1016/j.rsma.2022.102672

Abstract

The Caspian Sea (CS), biggest inland water worldwide has experienced around 3 m oscillation in sea level during the 20th century. These rapid sea level fluctuations have had a great impact on the coastal habitat around this sea. Therefore, this study is aimed to investigate the long-term changes of the western part of the Caspian Sea shoreline and Anzali lagoon and their dynamic responses to the sea level fluctuation using time series analysis of remotely sensed data over the 40-years. To this end, the long-term Caspian Sea shoreline and the area and perimeter of the Anzali Lagoon were extracted from the time series of Landsat satellite imagery (1975 till 2016) by using an automatic procedure including the combination of the Tasseled- Cap and texture filter methods. Afterwards, shoreline erosion/accretion rates were evaluated by using the Net Shoreline Movement (NSM) and End Point Rate (EPR) techniques. Finally, the sea level changes of the CS, were extracted through the multiple altimetry satellite data and the relationship between the relative sea level fluctuation and CS shoreline and Anzali lagoon area were studied. Results of the changes of shoreline positions over the study period (1975-2016) indicate that the whole coastal study area is subjected to accretion and erosion of 20.37 and -19.22 (m/year) respectively. There is balance between the whole EPR in all transects and periods between 1975 and 2016. This shows that when erosion happens in a region, accretion will be happened in another region, and this behavior is symmetrical. When the sea level decreased, the EPR values showed the accretion/seaward and vice versa. So, the shoreline movement has a strong nonlinear response to the sea level fluctuation with a coefficient of determination of −0.66. Also results show the strong response of the Anzali lagoon to the sea level fluctuation with a coefficient of determination of 0.78 for a nonlinear relationship between the changes of area of Anzali Lagoon and the CS fluctuation. This lagoon experienced the greatest and lowest values of its area on 2003 and 1985, respectively, which are matched with the high and low stands of the Caspian Sea Level.

Keywords : Shoreline change/Sea level/Remote sensing/Caspian Sea/Anzali lagoon

1. Introduction

Dense populations living along shorelines, especially in the developing countries, may leave communities vulnerable to flooding or other aspects of water level change (Al-Tahir and Ali, 2004).

Meanwhile, millions of people have confronted a serious threat (Arkema et al., 2013, Kirwan and Megonigal, 2013, Li and Gong, 2016) due to global mean sea level rise owning to ice melt and climate change in recent years (Nicholls and Cazenave, 2010, Webb et al., 2013, Yang et al., 2013). Moreover, unique habitat characteristics of coastal wetlands and lagoons made them as an important geographic areas and component of coastal area (Kuleli et al., 2011). The coastal lagoons and wetlands, generally as a shallow lake form in topographically low regions behind coasts, are hydraulically connected with the open sea water and are affected by the sea level fluctuation (Duck and Figueiredo da Silva, 2012). The type of this connection can affect the natural structure of the coastal wetlands and lagoons and the morphological and ecological conditions of the coastline (Ozturk and Sesli, 2015). Monitoring the dynamic of the coastal zones is an important task in national and sustainable coastal development and environmental protection (Kuleli et al., 2011, Liu et al., 2013). So, shoreline change detection and monitoring is important for coastal hazard assessment (Marfai et al., 2008).

For achieving this important issue, time series extraction and analysis of the shoreline's changes and coastal lagoons and wetlands and their relation with environmental parameters especially sea level changes is a great important (Bagli and Soille, 2003, Mills et al., 2005, Pardo-Pascual et al., 2012, Hamzeh et al., 2017). Despite the importance of monitoring the coastal areas, this task by using the traditional ground survey techniques is difficult and time-consuming due to the large extent and variability of these areas (Cracknell., 1999, (Hamzeh et al., 2017).

Satellite imagery with ability to project and map recent changes of shorelines (Shaghude et al., 2003) can provide fast, low cost and valuable estimation of coastal changes (Yang et al., 1999, Moussaid et al., 2015, Ozturk and Sesli, 2015). Therefore, in recent year remotely sensed data have been widely used and their capability and performance for coastal monitoring are confirmed in different studies (e.g. (Kuleli, 2005, Vanderstraete et al., 2006, Ekercin, 2007, Genz et al., 2007, Wu, 2007, Sesli et al., 2008, Bayram et al., 2008, Ghanavati et al., 2008, Rebelo et al., 2009, Kuleli, 2009, Maiti and Bhattacharya, 2009, Kuleli et al., 2011, Pardo-Pascual et al., 2012, Kakroodi et al., 2014b, Hamzeh et al., 2017, Jeihouni et al., 2019)). Also, availability of long time series of multispectral satellite imagery such as Landsat data and their global-scale coverage, has caused their preference in compared to other methods for coastline monitoring and change analysis (Pardo-Pascual et al., 2012, El-Asmar et al., 2013).

Several different remotely sensed methods are existing for semi-automatic and automatic extraction of shoreline and water bodies changes such as Tasseled Cap Transform (Scott et al., 2003, Jain et al., 2005, Ouma and Tateishi, 2006, Fisher et al., 2016), supervised and unsupervised classification (Soliman and Soussa, 2011, García-Rubio et al., 2015), Principal Component Analysis (Lira, 2006), single-band thresholds (Klein et al., 2014, Moser et al., 2014), band rationing and variety of different spectral indices such as Normalized Difference Water Index (NDWI) (McFeeters, 1996), Modified Normalized Difference Water Index (MNDWI) (Xu, 2006) and Automated Water Extraction Index (AWEI) (Feyisa et al., 2014). Among the mentioned methods, single-band density slicing, band rationing and indices have been mostly used due to their easier calculations (Alesheikh et al., 2007, Van and Binh, 2009, Feyisa et al., 2014). In general, all indices have been achieved overall accuracies of 95%–99% for pure pixels, and 73%–75% for mixed pixels.

While the fluctuation of global sea level is approximately 2 mm/year, the Caspian Sea (CS), biggest inland water worldwide with a surface area of 428,500 km^2 (the last size of CS was calculated by (Arpe et al., 2019)) has experienced a

3 m oscillation (same as Great Lakes in North America) in the same period during the 20th century (Kroonenberg et al., 2007, Kakroodi et al., 2012, Haghani et al., 2016). The CS level variation is complex, resulting from different processes and settings such as the relative impacts of hydro-climatic change, ice-sheet accumulation and melt, isostactic adjustment on the CS level, increasing the construction of dams along the Caspian drainage basin area, and southward redirection of north-flowing rivers (Koriche et al., 2022).

Technically and naturally similarity of CS to the lake and its'sea-like'- size lead to a unique opportunity and natural laboratory for assessing the long-term impacts of global sea level changes on the coastal environments in a short time frame (Kakroodi et al., 2015, Haghani et al., 2016). These huge and rapid sea level fluctuations, not only have impacted the global climate (Arpe et al., 2012, Farley Nicholls and Toumi, 2014), but also, they have affected on the coastal geomorphology changes including passive inundation, beach-ridge formation, barrier-lagoon development and general erosion (Kaplin and Selivanov, 1995, Naderi Beni et al., 2013, Kakroodi et al., 2014a). Furthermore, they have affected on the lives of more than 10 million people around the CS (Dolotov and Kaplin, 2005, Kosarev, 2005, Leroy et al., 2011) by flooding, land demolition and impacting on economy. So far, no research has been done on the long-term monitoring of the Caspian Sea coastal area and its relationship with the Sea level changes. Therefore, this study is mainly aimed to analysis the long-term changes of the western part of the Caspian Sea shoreline and Anzali lagoon and investigate the dynamic responses of these areas to the sea level fluctuation using time series analysis of different optical and altimetry remotely sensed data.

To this end, the automatic shoreline extraction approach by combing the Tasseled- Cap and Texture filter techniques was developed and applied on the available Landsat imagery of 40-years for continuous monitoring of the coastline dynamic and Anzali lagoon. Also, different altimetry data including Jason-1, TOPEX/Poseidon, and Jason-2/OSTM were employed to investigate the relationship between sea level fluctuation and shoreline changes.

2. Material and methods

2.1. Study area

The study area is located in the southwest of the Caspian Sea between 38° 26

– 37° 17 N and 48° 52 – 50° 14 E (Fig. 1). Along this coastline lye various cities, settlements, agricultural fields, forest and natural resources. The Anzali Lagoon, largest freshwater reservoir of the Southern Caspian Sea, is located at the eastern part of this region between 37° 35 – 37° 26 N and 49° 15 – 49° 27 E. This famous wetland certificated as one of the first Ramsar sites in the world in June 1975 and is known as an important habitat for various species of birds and fish. This lagoon is a coastal wetland and is connected to the Caspian Sea by a navigable channel through the two wave-breaker located in Anzali port facilities. In recent years, due to transfer the different factor including the sea level changes, climate change, anthropogenic activities and feeding sediment from rivers into this lagoon, the depth and areas of this lagoon has been declined every year. Average depth of wetland has dropped from 14 meters to 2 meters in the past 30 years and recently, it is approximately reached to below 1 m.

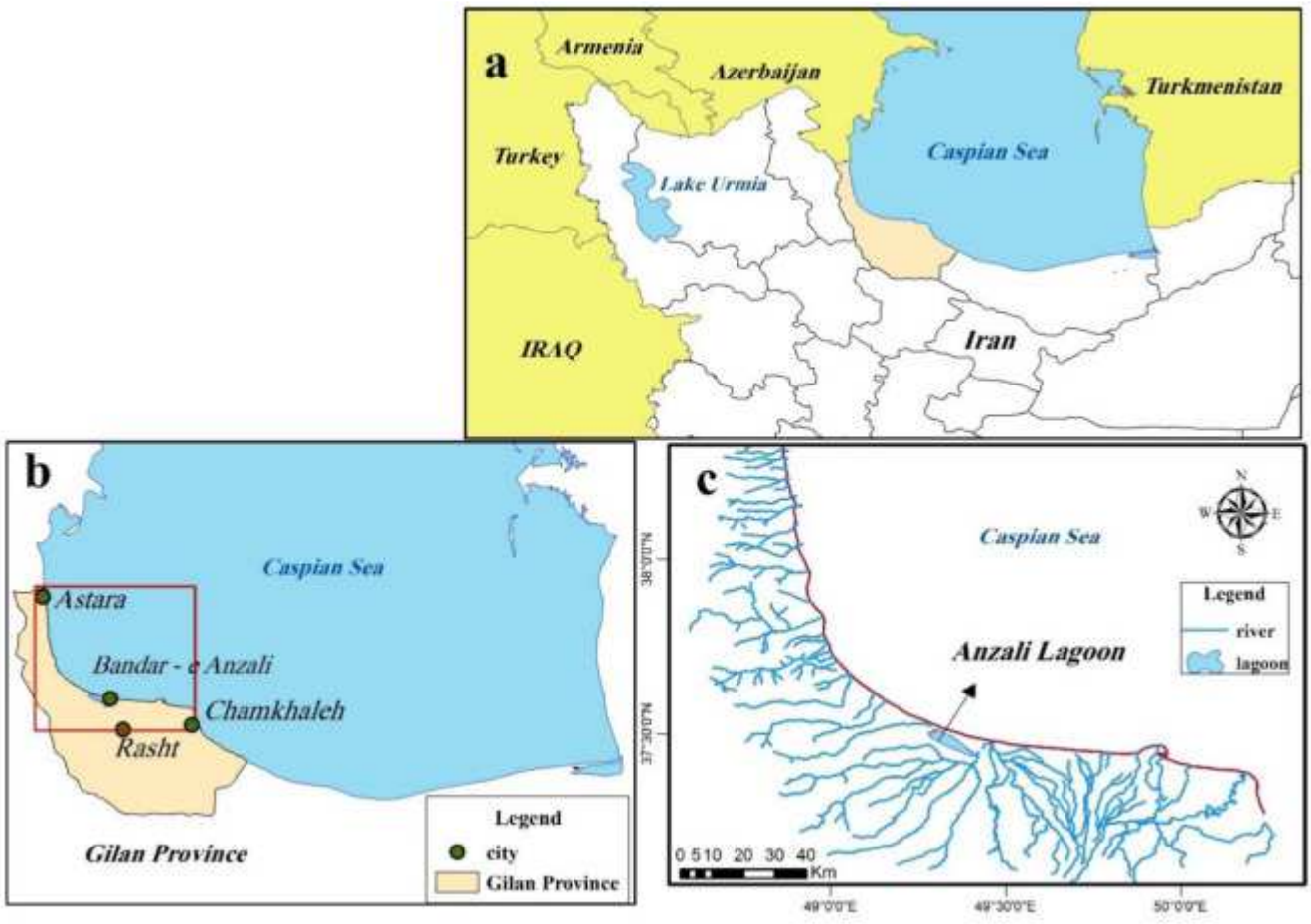

Fig. 1. Location of the selected study area along the south west of Caspian Sea (b), and Anzali Lagoon (c).

2.2. Remote sensing data

2.2.1. Landsat multispectral data

In this study, Landsat multispectral satellite imagery for a period of 42 years (1975–2016) were used to extract the shoreline and lagoon changes along the study area. For each year an image during the months of June till September from the Landsat MSS (Multi spectral Scanner), TM (Thematic Mapper), ETM+ (Enhanced Thematic Mapper) and OLI (Operational Land Imager) imagery with cloud cover <30% were selected and downloaded from the United States Geological Survey Center for Earth Resources Observation and Science (USGS/EROS). Moderate temporal frequency and medium spatial resolution of Landsat imagery, 16 days and 30 m respectively, have made potential usefulness than other data sources for monitoring coastline dynamics at large areas (Li and Gong, 2016). In total twenty-one images were acquired from Landsat satellites series. The acquisition date and name of satellites and sensors are summarized in Table 1.

All images were downloaded at Level-one Terrain-Corrected (L1T) images. These products are geometrically calibrated by using both ground control points (GCP) and digital elevation models (DEM) and with Universal Transverse Mercator (UTM) coordinate transformation (NASA, 2006) with an accuracy of more than 0.44 pixels (13.4 m), which make them trusted for pixel-level time-series analysis. Then necessary image preprocessing including the layer stacking of optical bands, converting the DN values into at satellite radiance values and then converting the radiance values into surface reflectance values by using the quick atmospheric correction (Bernstein et al., 2012) were applied on all of the

images. Meanwhile, the MSS images were resampled to 30 m resolution using the nearest neighbor method for matching their spatial resolution with other Landsat series.

Table 1. List of Landsat data used in this study.

No	Date	Satellite- sensor	Spatial resolution (m)
1	1975.07.27	Landsat 2 -MSS	60
2	1978.07.29	Landsat 2 -MSS	60
3	1985.06.13	Landsat 5 -MSS	60
4	1987.08.06	Landsat 5 -MSS	60
5	1989.07.02	Landsat 4 -TM	30
6	1993.07.21	Landsat 5 -TM	30
7	1998.06.17	Landsat 5 -TM	30
8	1999.08.23	Landsat 5 -TM	30
9	2001.08.20	Landsat 7 -ETM+	30
10	2002.08.07	Landsat 7 -ETM+	30
11	2003.05.06	Landsat 7 -ETM+	30
12	2006.08.10	Landsat 5 -TM	30
13	2007.08.29	Landsat 5 -TM	30
14	2008.06.12	Landsat 5 -TM	30
15	2009.10.21	Landsat 5 -TM	30
16	2010.06.02	Landsat 5 -TM	30
17	2011.06.05	Landsat 5 -TM	30
18	2013.10.16	Landsat 8 OLI	30

No	Date	Satellite- sensor	Spatial resolution (m)
19	2014.08.16	Landsat 8 OLI	30
20	2015.06.16	Landsat 8 OLI	30
21	2016.08.05	Landsat 8 OLI	30

2.2.2. Altimetry satellite data

Relative Caspian Sea level variations were extracted from the data provided by the TOPEX/POSEIDON (T/P), Jason-1 GDR-C 20hz altimetry and Ocean Surface Topography Mission (OSTM)/ Jason-2 Interim GDR 20hz satellite altimetry and used for assessment the influence of sea-level change on Caspian Sea shoreline and perimeter of the Anzali lagoon changes during the study period. These data were downloaded from the USDA.gov altimetry datasets (https://www.pecad.fas.usda.gov/cropexplorer/global_reservoir/). Fig. 2 shows the Caspian Sea height variations in date by considering the day and month of Landsat satellite imagery which used in this research.

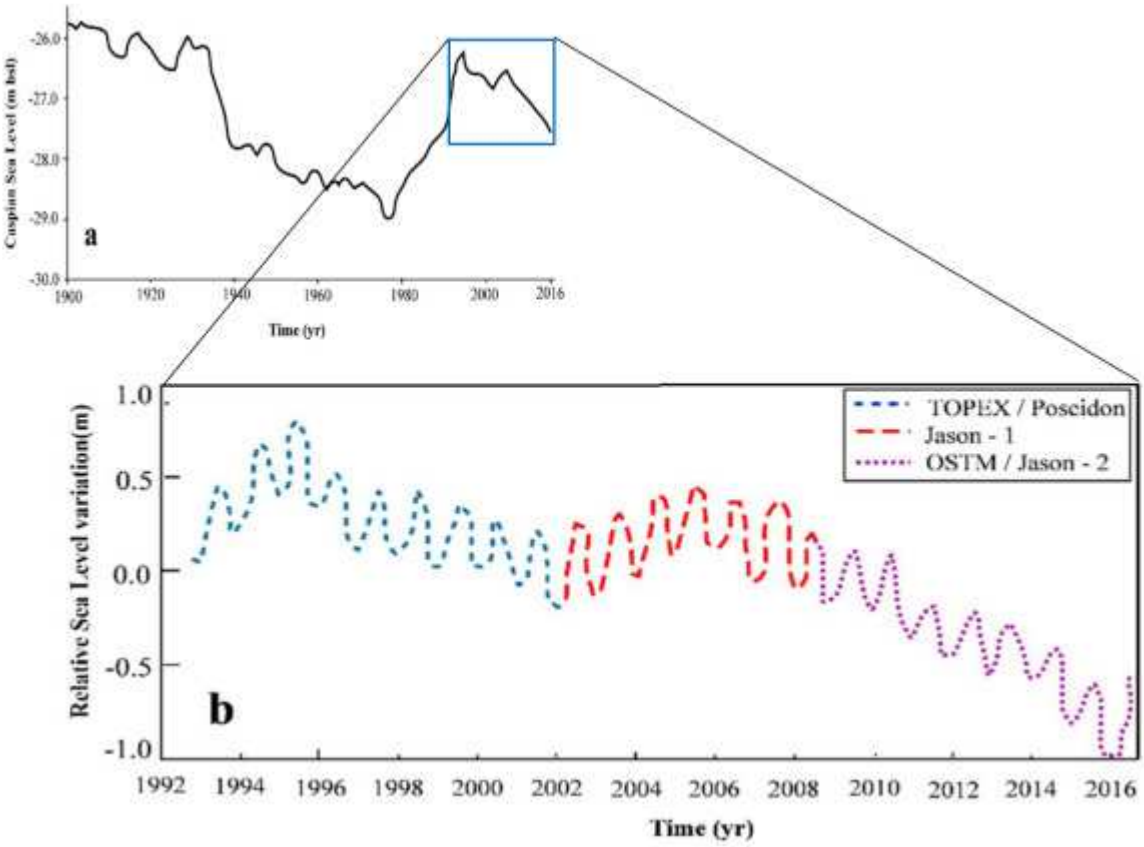

Fig. 2. (a) Caspian Sea level (CSL): 1900 to 1992 (Arpe et al., 2000, Arpe et al., 2020); and 1992 to 2016 from. (b) Relative Caspian Sea level variation from 1993 to 2016 based on satellite radar altimetry data (USDA, 2016).

2.3. Methodology

In this study, an improved methodology was performed for extraction the CS shoreline and water body of Anzali lagoon during last 42 years and determine the net rate of shoreline movement and perimeter changes of the lagoon and their relationship with relative sea level fluctuation. The methodology can be defined in three steps including the (1) preprocessing of Landsat satellite imagery and apply the appropriate approach for shoreline and water body extraction (2) change detection evaluations to compute shoreline erosion/accretion rates and lagoon expansion and shrinkages and (3) assessment the response of these changes to Caspian Sea level fluctuation during the years of 1992 till 2016. The methodology of the study is summarized in the presented flowchart in Fig. 3, and is explained in details in following.

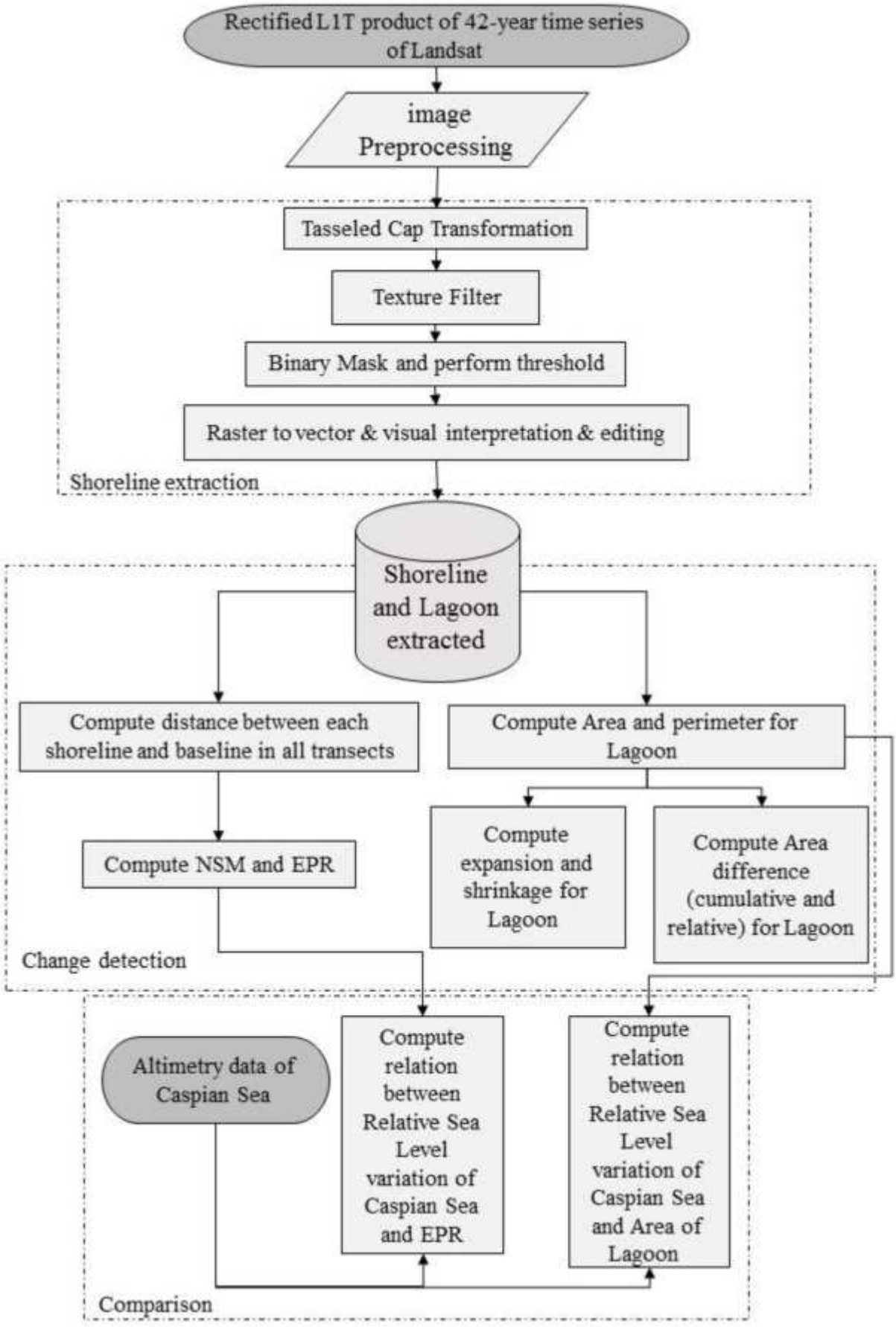

Fig. 3. Workflow scheme showing the main steps of the study.

2.3.1. Shoreline extraction

In this study, the combination of Tasseled Cap Transformation (TCT), Texture Filter and apply appropriate thresholds was suggested for extracting the shorelines and water bodies from Landsat imagery. The Tasseled Cap Transformation were originally developed based on spectral measurements and analysis of wheat growth by Kauth and Thomas (1976). The Tasseled Cap Transformation linearly combines the Landsat bands in order to create three principal components including brightness, greenness and wetness in order to differentiate between land, water, and vegetated areas by using of coefficients derived with sampling known land cover spectral characteristics (Scott et al., 2003). The TCT coefficients determine based on a graph between Red and Near Infrared (NIR) wavelengths. In this study, the coefficients for Tasseled Cap Transformation of Landsat data were derived from Kauth et al. (1979), Crist (1985), Huang et al. (2002) and Baig et al. (2014) (Table 2) for MSS, L5, L7 and L8 satellite imagery respectively.

After apply the TCT on each image, the Texture Filter has been applied on the output of TCT for easily and more accurately detecting the shorelines. The texture filter made discrete areas which are more homogeneous rather than areas having a different texture. After performing this process, its output was converted to binary image and appropriate thresholds were applied on them for extracting the shoreline. The threshold has been interactively (with manual trial-and-error procedure) adjusted and also evaluated until obtaining satisfied results (Singh, 1989). Then the shoreline boundary was extracted and evaluated with some high spatial resolution data form the google earth for improving the accuracy of final outputs.

Table 2. Landsat Tasseled Cap coefficients for Landsat MSS, TM, ETM and OLI top of atmosphere reflectance values.

Sensor-index	Band coefficients						Reference
	F_{Blue}	F_{Green}	F_{Red}	F_{NIR}	F_{SWIR1}	F_{SWIR2}	
MSS -TCB		0.332	0.603	0.675	0.262		Kauth et al. (1979)
MSS- TCG		−0.283	−0.66	0.577	0.388		
MSS- TCW		−0.899	0.428	0.076 0.5741	0.041		
L5 -TCB	0.2043	0.4158	0.5524	0.7940	0.3124	0.2303	Crist (1985)
L5- TCG	−0.1603	−0.2819	−0.4934	0.1594	−0.0002	−0.1446	
L5- TCW	0.0315	0.2021	0.3102	0.6966 0.6966	−0.6806	−0.6109	
L7 -TCB	0.3561	0.3972	0.3902	0.0656	0.2286	0.1596	Huang et al. (2002)
L7- TCG	−0.3344	−0.3544	−0.4556	0.5599 0.7276	−0.0242	−0.2630	
L7- TCW	0.2626	0.2141	0.0926	0.3407	−0.7629	−0.5388	
L8 -TCB	0.3029	0.2786	0.4733		0.5080	0.1872	Baig et al. (2014)
L8- TCG	−0.2941	−0.243	−0.5424		−0.0713	−0.1608	
L8- TCW	0.1511	0.1973	0.3283		−0.7117	−0.4559	

2.3.2. Change detection of Caspian Sea shoreline and Anzali Lagoon

The Federal Emergency Management Agency (FEMA) has established the transect assessment from baseline approach for evaluating long term coastal change rates (Crowell et al., 1991). Therefore, this approach was used in this study. For this purpose, transect single baseline was traced distance to the shorelines based on the buffer method. Then, these transects have been created in perpendicular to the baseline in an interval of 5 km from Astara to Chamkhaleh cities. Along the Sefid Rud Delta due to the rapid variability of shoreline, this interval was taken to be 2 km. Then, the distance between the shoreline of different years and baseline in all transect has been measured orthogonally. Afterwards, shoreline erosion/accretion rates or changes of the shoreline position were computed by using the Net Shoreline Movement (NSM) and End Point Rate (EPR) techniques. The EPR method is the most prevalent technique among other methods for calculating the shoreline movement rates, and it is widely used in different coastal researches (Dolan et al., 1991, Thieler et al., 2005, Genz et al., 2007, Ford, 2013, Ozturk and Sesli, 2015, Kermani et al., 2016). The NSM simply; indicates a distance (in meters) between the oldest and new shorelines position in each transect (Manca et al., 2013, Kermani et al., 2016). The EPR indicates the annual rate of change (m/ year) by dividing the distance (in meters) separating two shorelines by the differences of dates of the two shorelines (Eq. (1)) (Kermani et al., 2016). (1) Where: D1 and D2 are distance which separating the shoreline and baseline, and are the dates of two shoreline positions.

Landward displacement of the shoreline or erosion feature was indicated by the negative value of EPR and NSM values. While seaward migration or accretion feature was denoted by their positive value (Kermani et al., 2016). The obtained erosion/accretion rates for western Caspian Sea coastline were

divided into seven categories based on expert experiences. But for illustrating the importance of the study area, we compared this category with Natesan et al. (2015) which have been widely used in other researches. Table 3 shows these cooperation and different defined categories based on this classification approach.

As another part of the study to analysis the changes of the Anzali Lagoon, after extracting the water body of this logon during the study period, it was converted to the separate polygon for each year and then area and perimeter of this lagoon were calculated for each year and then both spatially and quantitatively assessment from that was performed. Furthermore, the spatial detection of areas of lagoon expansion and shrinkage was performed for a time periods of 1975–1985, 1985–1993, 1993–2003, 2003–2008, 2008–2011, 2011–2016 and 1975–2016.

Table 3. Shoreline classification based on EPR and statistics of EPR in all transects and years.

S. no.	**Rate of shoreline change of the world (m/year)**	**Shoreline classification**	**Statistics of EPR of the study area**		**S. no.**	**Rate of shoreline change (m/year)**	**Shoreline classification**
1	>−2	Very high erosion	Min	−370.94	1	> −200	Very high erosion
2	>−1< −2	High erosion	Max	289.81	2	> −200< −100	High erosion
3	>−1< 0	Moderate erosion	Mean	−1.26	3	>−100< 0	Moderate erosion
4	0	Stable	Std.	35.83	4	0	Stable
5	>0 < +1	Moderate accretion			5	>0 < +100	Moderate accretion
6	>+1< +2	High accretion			6	>+100< +200	High accretion
7	>+2	Very high accretion			7	>+200	Very high accretion

At the end, in order to evaluate the effect of sea level changes on the CS shoreline and Anzali lagoon, the relationship between EPR for shorelines and areas of Lagoon with the relative Sea Level changes were investigated.

3. Results and discussion

3.1. The Caspian Sea shoreline changes between Astara and Chamkhaleh regions

Information on shoreline changes and movement based on the EPR are provided in Fig. 4. The positive and negative values of the EPR displayed in the following figure indicate seaward/accretion and landward/erosion areas, respectively. The maximum changes have occurred in 1985–1987, 1987–1989 and 2002–2003 periods. In transects belong to the Sefid Rud delta, the maximum EPR have been achieved especially in 1987–1989, 1989–1993, 1993–1998, 1999–2001, 2007–2008 and 2009–2010 periods. Based on (Natesan et al., 2015) classification for EPR, most of transects are belong to very high category.

The spatial and statistical results of the shoreline evolution (erosion and accretion) for three periods of time (1978–1985, 2003–2006, 2015–2016) along the whole study area with more detail for each region (important cities along the study area) are shown in Fig. 5, Fig. 6, Fig. 7. These figures include the mean of NSM and EPR in Astara-Landvil, Choobar – Khotbeh Sara, Lisar – Asalem, Paresar port- Rezvanshahr, Bandar Anzali, Bandar Anzali-Haji Bekandeh, sefid Rod Delta-Kiashahr Port and Dehgah – Chamkhaleh regions.

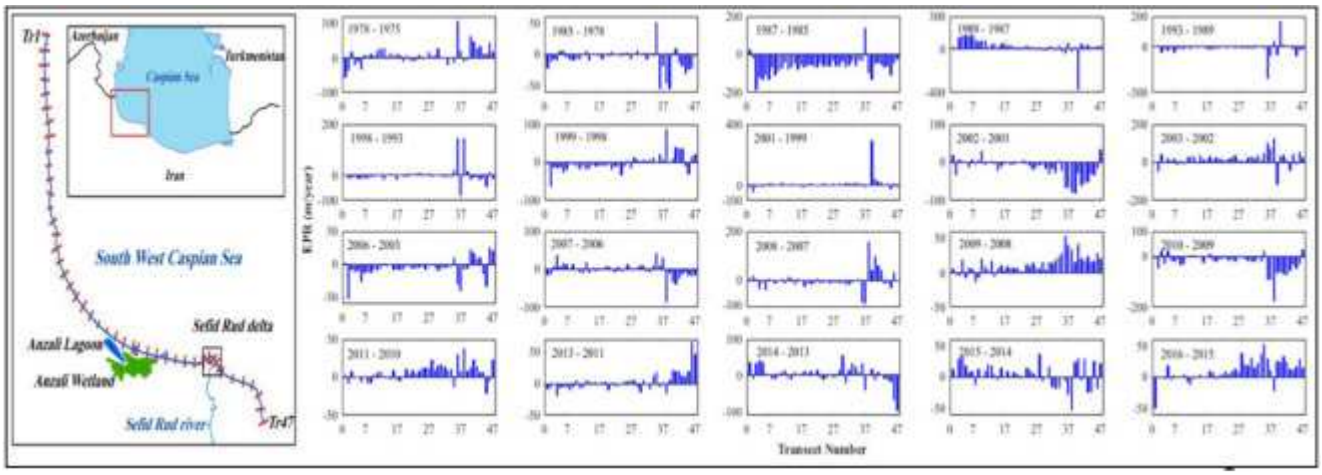

Fig. 4. EPR of the shoreline of Caspian Sea in all transects between 1975 till 2016.

The coast experienced even seaward migration or landward erosion due to local factors, such as sediment supply, wave energy, lateral sedimentation transport, and other coastal morphology factors. During sea-level rise it might erode in some part and transfer somewhere else through current long shore as observed at some parts, due to this there is always a balance in the coastline by accretion and erosion imposed by sea-level change.

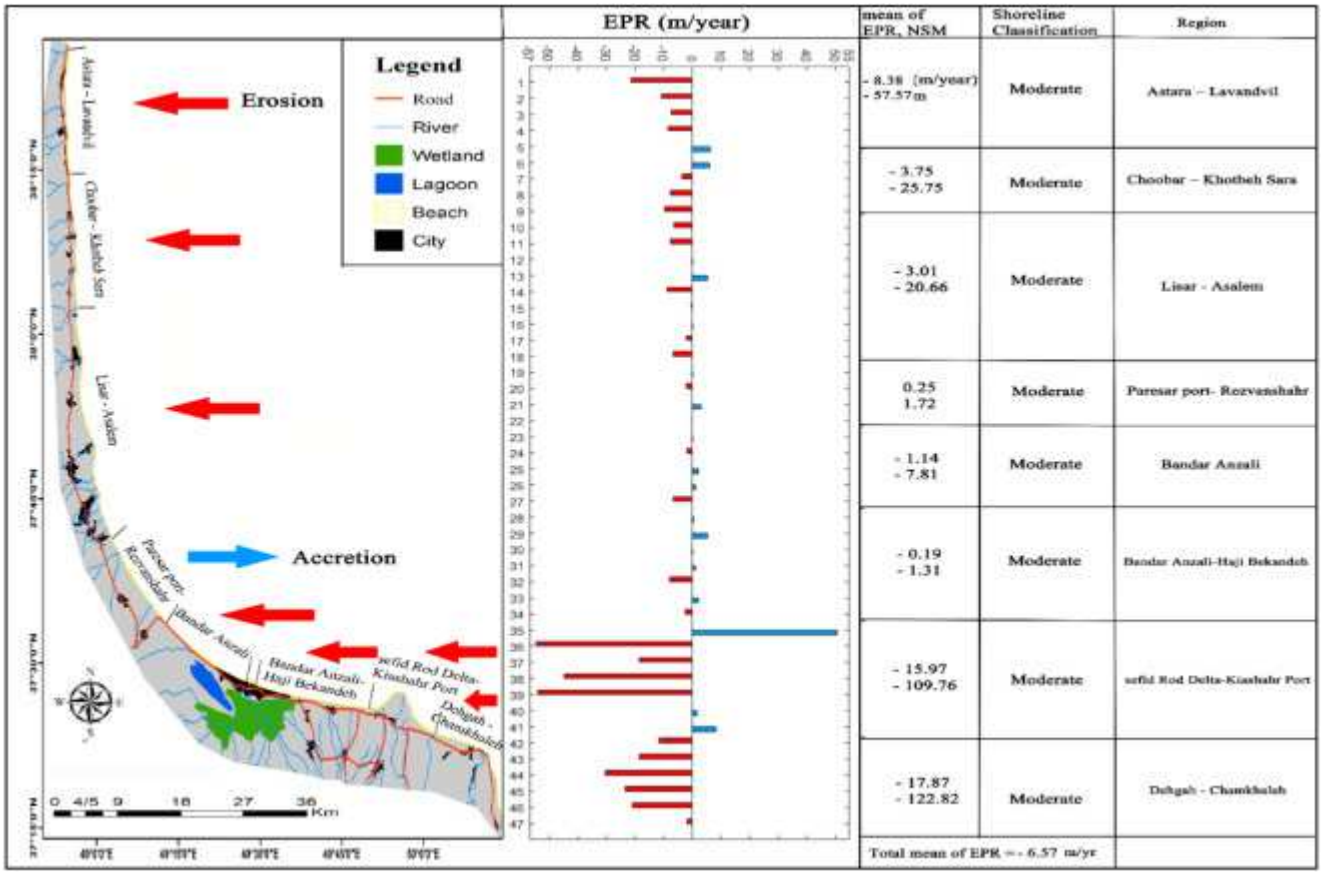

Fig. 5. Shoreline evolution (erosion and accretion) between 1978 till 1985 computed by the EPR.

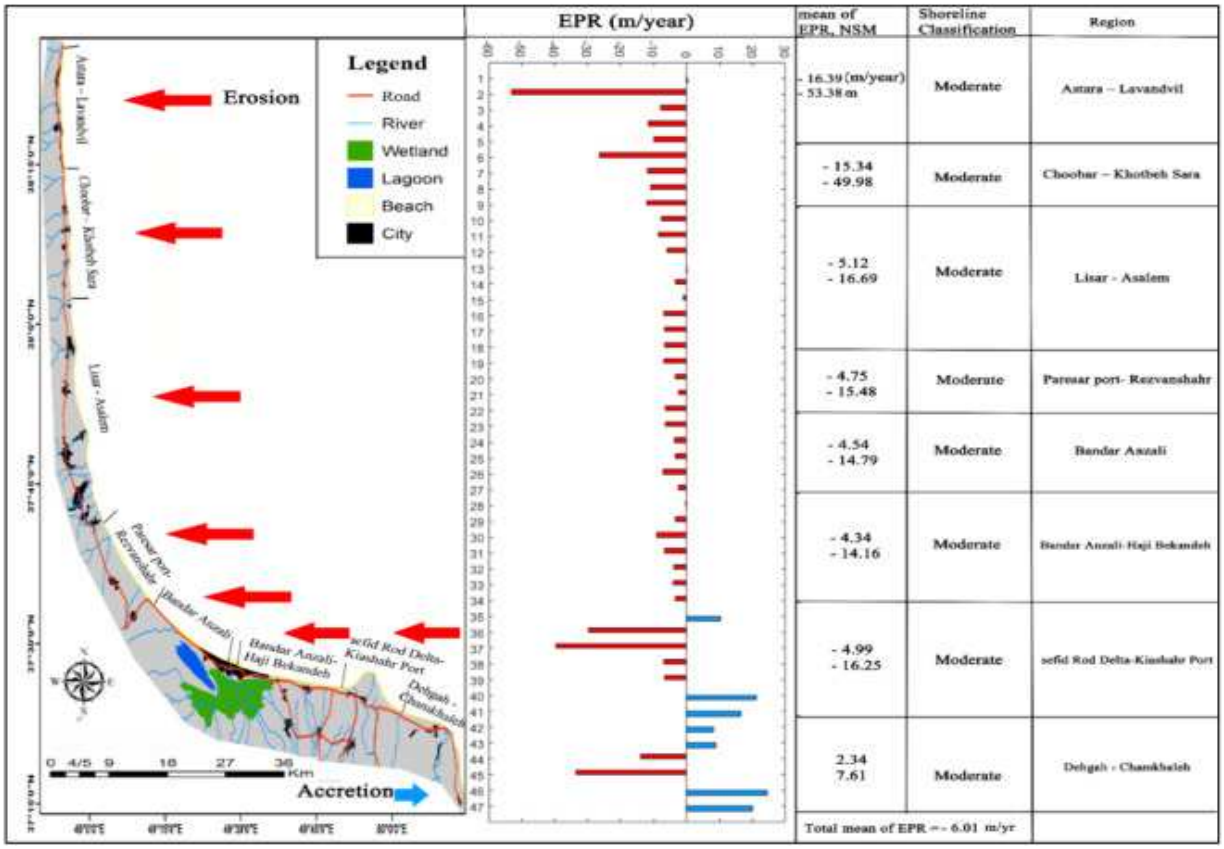

Fig. 6. Shoreline evolution (erosion and accretion) between 2003 till 2006 computed by the EPR.

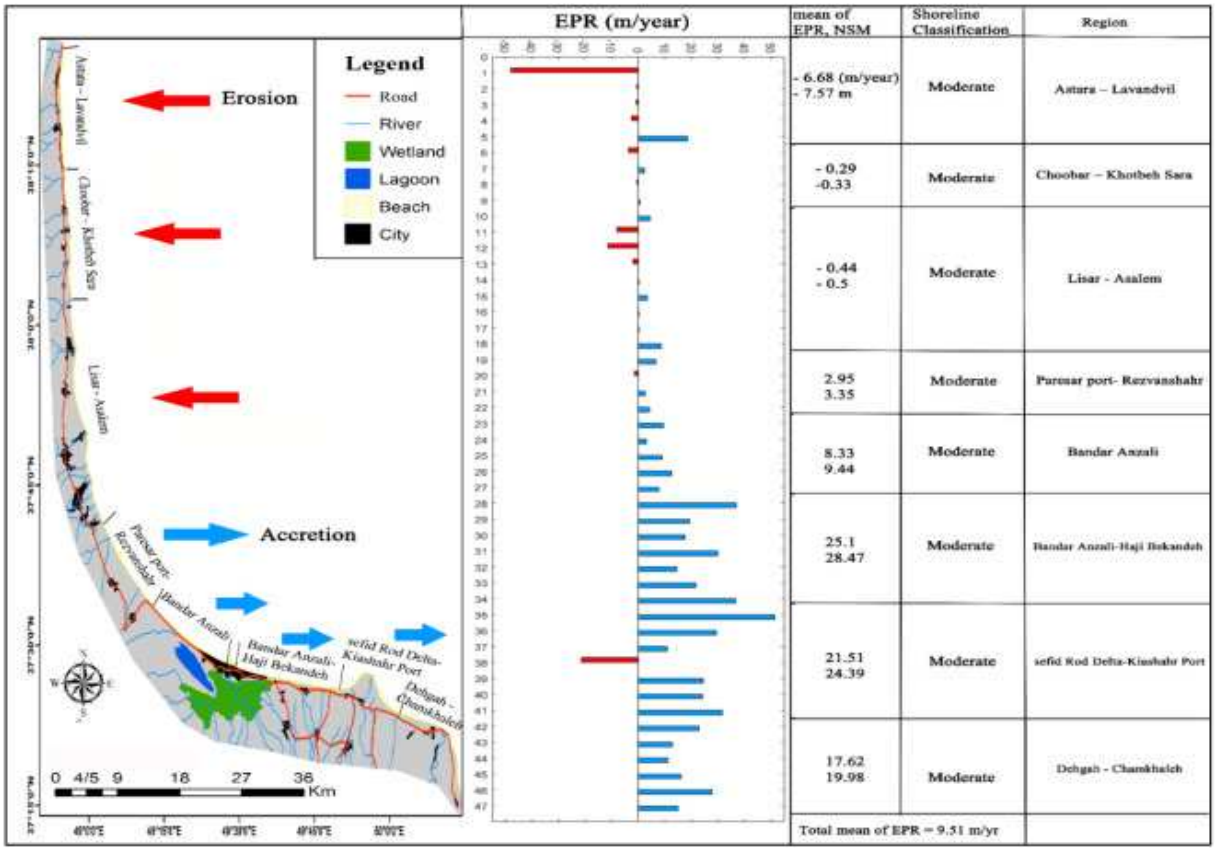

Fig. 7. Shoreline evolution (erosion and accretion) between 2015 till 2016 computed by the EPR.

Therefore, the results showed shorelines located at Astara-Landvil, Choobar – Khotbeh Sara and Lisar – Asalem regions had erosion in all periods while accreting shorelines are observed at Paresar port-Rezvanshahr region in these periods except 2003–2006 period. Maximum erosion rates of −15.97 and −17.87 (m/year) are observed at Sefid Rod Delta-Kiashahr Port and Dehgah – Chamkhaleh regions for a period of 1978–1985 respectively. In this period, shorelines have confronted erosion at all regions except Paresar port- Rezvanshahr region by EPR of 0.25 (m/year). While, during 2003–2006, shorelines of Astara-Landvil and Choobar – Khotbeh Sara have experienced maximum erosion rates of −16.39 and −15.34 (m/year). Also, in this period, erosion have been observed in all regions except Dehgah – Chamkhaleh region by 2.34 (m/year) from EPR rates. During 2015–2016 period, the coastline has experienced more accretion than erosion by maximum value of 25.1 and 21.51 (m/year) in Bandar Anzali-Haji Bekandeh and sefid Rod Delta-Kiashahr Port region, respectively. While, the maximum rate of erosion is recorded to be −6.68 (m/year) EPR rate at Astara-Landvil region.

The mean changes of shoreline positions over 1975–2016 period indicate that the whole coastal study area is subject to accretion and erosion of 20.37 and −19.22 (m/year) respectively. There is balance between the whole EPR in all transects and periods between 1975 and 2016. This shows that when erosion was happened in a region, accretion will happen in another region, too, and this behavior is symmetrical.

3.2. The relationship between shoreline changes and sea level fluctuation

The average EPR values and relative sea level fluctuation is illustrated in Fig. 8. Based on this figure, when the sea level decreased, the EPR values showed the accretion/seaward more than erosion/landward. While, in periods that sea level has increased (in 2001–2002, 2006–2007 and 2009–2010), the EPR values showed the erosion/landward more than accretion/seaward. The maximum rate

of changes of coastline is belong to 1985–1987 and 1987–1989. During these periods, the coastline experienced the −64.19 and −52.06 (m/year) erosion, and 82.08 and 42.29 (m/year) accretion, respectively. So, the shoreline and coastline movement have a strong response to the sea level fluctuation. The relationship between the sum of seaward and landward with relative sea level changes during the study period is given in Fig. 9. As it can see, there is a nonlinear relationship between them with the strong opposite correlation (R −0.66).

Also, the EPR results of six transects along the Sefid Rud delta versus Relative Sea Level Change for a period of 1975 till 2016 is illustrated in Fig. 10. The results indicate that there is a very weak correlation (, −0.31, −0.36, −0.31, −0.3 and −0.34) between EPR and sea level change on this region. In fact, in this delta, the oscillation of sea is not correlated to sea level variation due to the high value of sedimentation in this region.

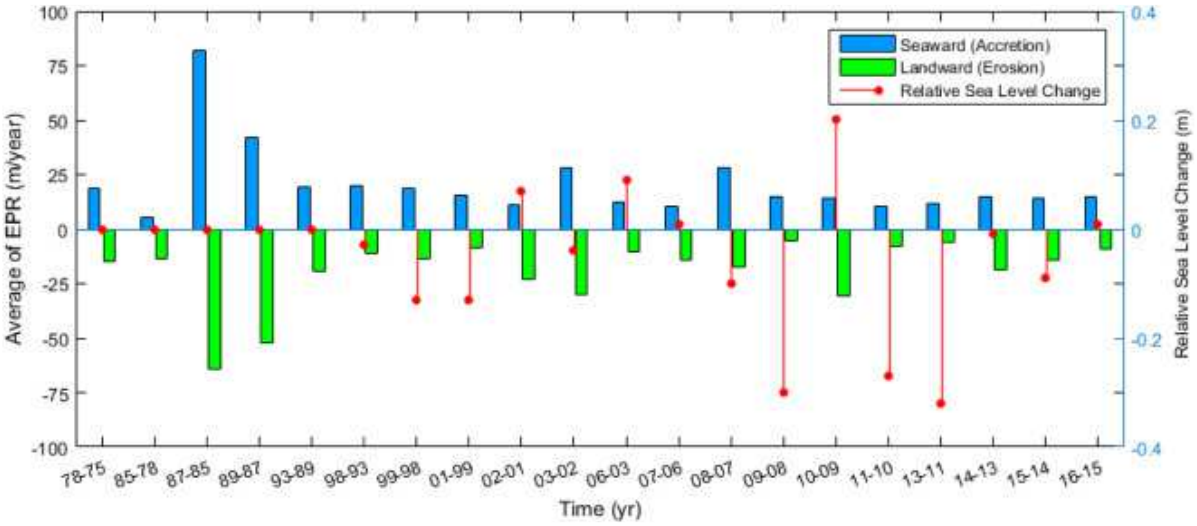

Fig. 8. Average of EPR versus sea level change along the study area between 1975 till 2016.

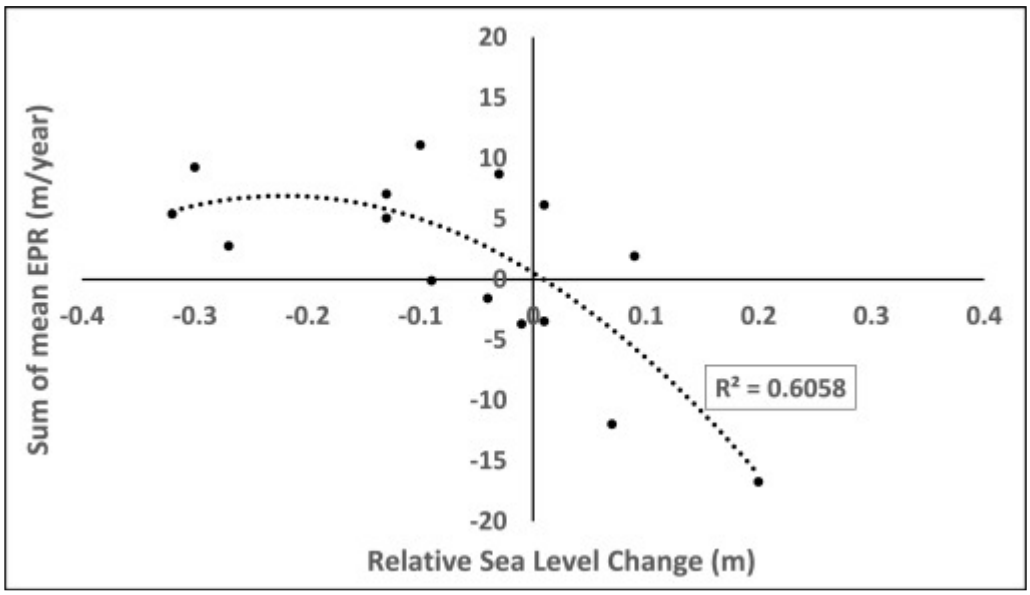

Fig. 9. Correlation between the sum of seaward-landward and relative sea level variation between 1993 till 2016.

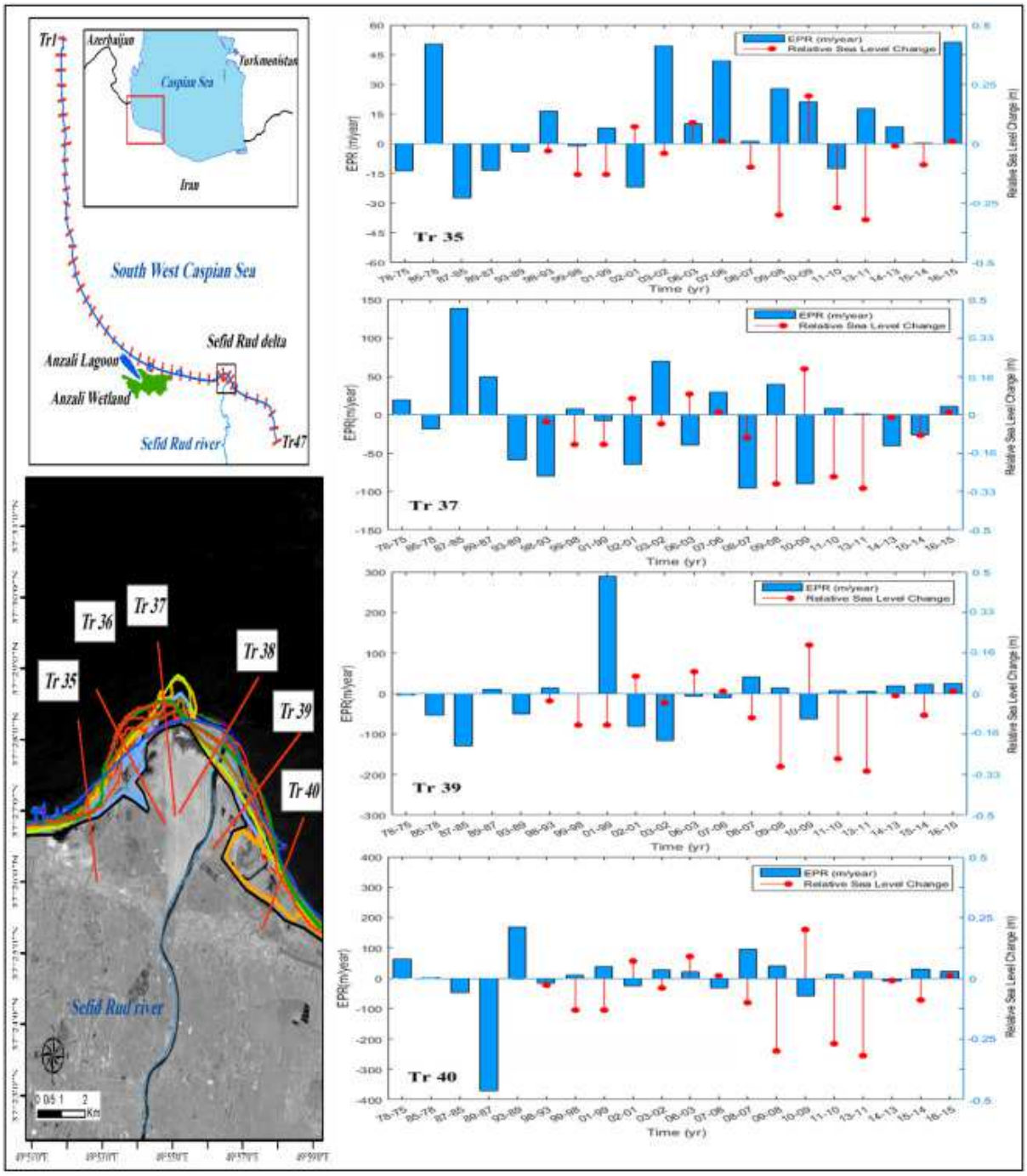

Fig. 10. Average of EPR versus sea level change between along the Sefid Rud Delta during 1975 till 2016.

3.3. Anzali Lagoon changes

The temporal changes in the area and perimeter of the Anzali Lagoon for a period of 1975 to 2016 is given in Table 4. The Anzali Lagoon experienced the greatest and lowest value in terms of the area at 2003 and 1985, respectively. Which, in these years the high-stand and low-stand of the Caspian Sea Level were happened during the study area. Therefore, it shows the strong response of the Anzali lagoon to the sea level fluctuation. This Lagoon has confronted the greatest and lowest value in terms of the perimeter at 1985 and 2011, respectively.

The spatial variability of the Lagoon expansion (land loss) and shrinkage (land gain) for a periods of 1975–1985, 1985–1993, 1993–2003, 2003–2008, 2008–2011 and 2011–2011 and overlay 1975–2016

were calculated and presented in Fig. 11. Also, overall spatial shrinkage and expansion areas of the Anzali lagoon during 1975 till 2016 is presented in Fig. 12.

Table 4. Perimeter and area of Anzali Lagoon and their changes between 1975 till 2016.

Yr.	**Area (km^2)**	**Perimeter (km)**	**Perimeter changes**	**Area changes**		
Empty Cell	Empty Cell	Empty Cell	Empty Cell	**Cumulative to 1975**	**Year by year**	**Event years**
1975	37.28	51.22				
1978	37.23	45.39	−5.83	−0.05	−0.05	
1985	26.09	57.52	6.29	−11.19	−11.14	−11.19
1987	34.92	55.02	3.79	−2.36	8.83	
1989	38.18	44.59	−6.63	0.90	3.26	
1993	37.52	45.23	−5.99	0.25	−0.66	11.44
1998	37.94	44.35	−6.88	0.66	0.41	
1999	37.44	42.75	−8.47	0.16	−0.49	
2001	37.77	45.33	−5.89	0.49	0.33	
2002	37.18	47.92	−3.3	−0.10	−0.59	
2003	39.74	51.11	−0.12	2.46	2.56	2.21
2006	35.76	48.05	−3.17	−1.52	−3.98	
2007	36.49	44.81	−6.41	−0.78	0.74	
2008	36.75	44.89	−6.32	−0.52	0.26	−2.99
2009	36.09	47.08	−4.15	−1.18	−0.66	
2010	36.85	50.78	−0.44	−0.43	0.75	

Yr.	Area (km^2)	Perimeter (km)	Perimeter changes	Area changes		
Empty Cell	Empty Cell	Empty Cell	Empty Cell	**Cumulative to 1975**	**Year by year**	**Event years**
2011	35.43	42.38	−8.84	−1.85	−1.42	−1.32
2013	34.51	49.61	−1.62	−2.77	−0.92	
2014	34.56	44.17	−7.05	−2.71	0.06	
2015	34.31	44.46	−6.76	−2.97	−0.25	
2016	32.95	48.19	−3.03	−4.33	−1.36	−2.48

An evaluation of the annual rates revealed that the maximum annual shrinkage (1.14 km^2/year) and expansion (1.46 km^2/year) rates occurred in the Lagoon during the 1985–1993 and 1975–1985 respectively, which agree with the sea level decreasing and increasing rates in these periods (Fig. 2). According to Fig. 11, the expansion rates of the Lagoon were more than its shrinkage before year 2003 and after this year following the decreasing of the sea level the rate of shrinkage in the Lagoon were more than expansion till 2016 and it seems that this trend will be continued till changing the sea level fluctuation rate. Therefore, it can be concluded that the area of the Anzali lagoon is strongly affected by the variation of the Caspian Sea level.

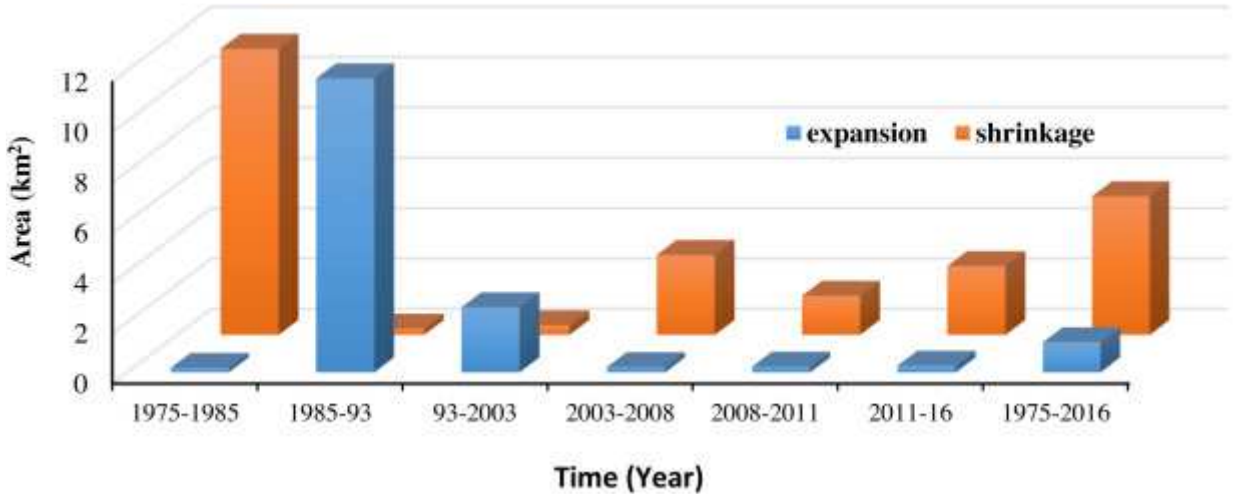

Fig. 11. Shrinkage and expansion area of the Anzali Lagoon between 1975 till 2016.

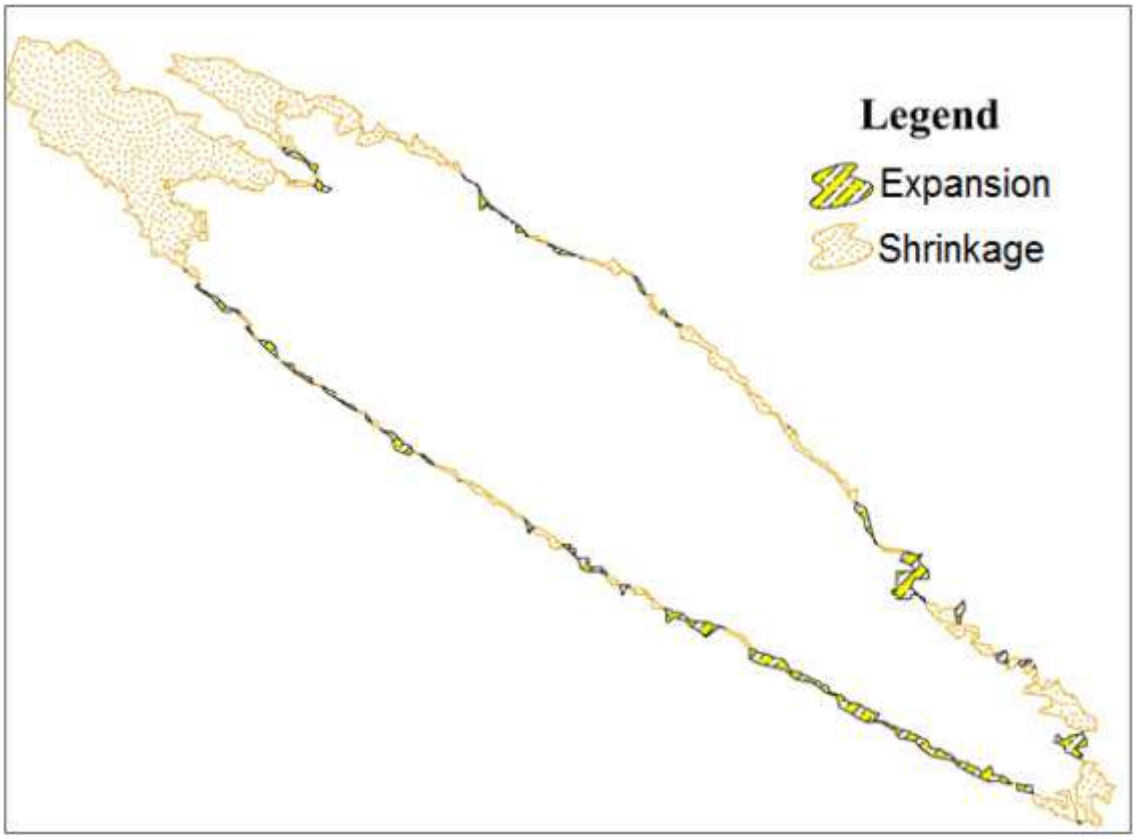

Fig. 12. Overall spatial shrinkage and expansion of the Anzali Lagoon during 1975 till 2016.

3.4. Relationship between the Anzali Lagoon changes and Caspian Sea level fluctuation

The variability of the Anzali Lagoon area between 1975 and 2016 versus Caspian Sea Level fluctuation are given in Fig. 13. It shows that Caspian Sea experienced the lowest and greatest relative sea level variation values of −0.59 and ＋0.46 in 2015 and 1993 respectively, during the study period. While the overall trend of sea level is descending, the insignificant ascending trends were happened in 2001–2002, 2003–2007, 2009–2010 and 2015–2016. In all of these periods, the area of Lagoon has been decreased except 2006–2007 and 2009–2010. Also, the linear and nonlinear relationship between the area of the Anzali lagoon and relative area level variation of Caspian Sea between 1993 and 2016 were calculated and are given in Fig. 14.

Based on the presented results in Fig. 14, there is a positive correlation between area of Lagoon and fluctuation of CS with a coefficient of determination of 0.78 and 0.69 for linier and nonlinear relationship respectively. It shows that this lagoon is strongly affected by the Sea level fluctuation and also in addition to the effect of sea level variation, another environmental factors such as precipitation, create dam on the river and also anthropogenic activity are led to the changes of this lagoon.

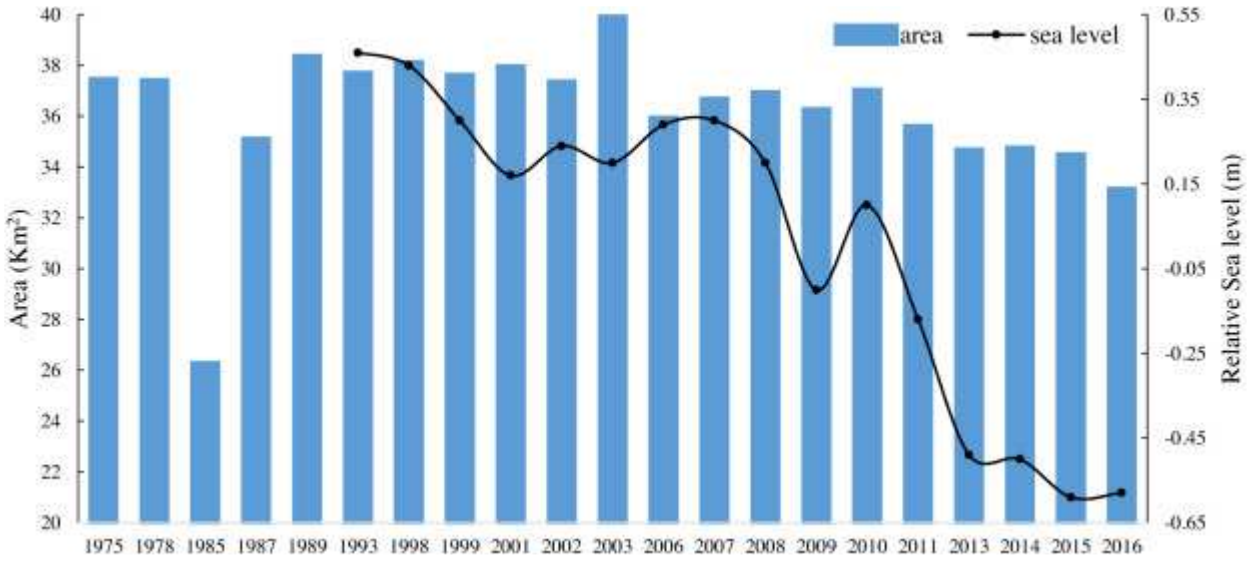

Fig. 13. Area of the Anzali Lagoon between 1975 and 2016 versus Caspian Sea level variation.

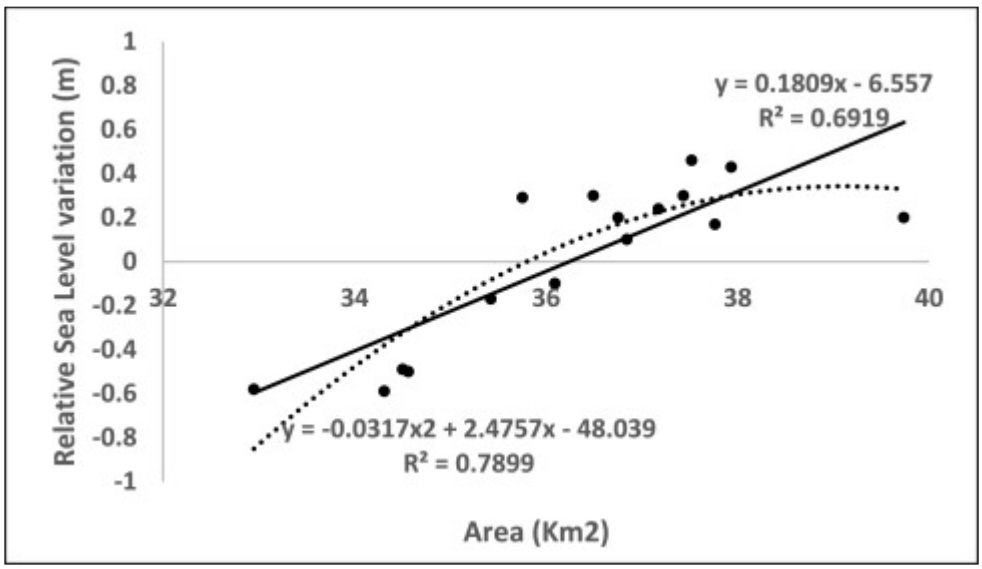

Fig. 14. Correlation between area of the Anzali Lagoon and relative sea level variation of Caspian Sea between 1993 and 2016.

4. Conclusion

In this study the long term (42 years) changes of the Caspian Sea shoreline and area of Anzali lagoon and their responses to the Caspian Sea level fluctuation were investigated using the time series analysis of Landsat satellite imagery and altimetry data of Jason-1, TOPEX/Poseidon, and Jason-2/OSTM. It was observed that the Caspian Sea has experienced an approximately 2 m oscillation during the last 30 years. As a result of this rapid and huge sea level fluctuations of CS, the shoreline, coastal area and lagoons next to this environment have experienced lots of changes and they are completely affected by this sea level fluctuation. There is a strong nonlinear correlation between rate of sea level and shoreline changes as well as area of Anzali lagoon. Results indicate the great capability of satellite data for monitoring of coastal area. Therefore, results of this study explain why in the context of global climate change, future sea level rise could accelerate the erosion of beaches around the world. This issue should be taken into account in future IPCC simulations. At the end we recommend the doing study on the

modeling the behavior of coastal area and lagoons in response to both changes in their upper catchments and sea level fluctuation and obtain the exact effect of these parts separately.

Declaration of Competing Interest

The authors declare that they have no known competing financial interests or personal relationships that could have appeared to influence the work reported in this paper.

Acknowledgment

This work has been supported by Center for International Scientific Studies & Collaboration (CISSC), Ministry of Science, Research and Technology of Iran and Cooperation and Cultural Activities (SCAC) section of the French Embassy in Iran under the Gundishapur program. The authors would like to kindly acknowledge the CISSC and French Embassy in Iran for their support.

Data availability

Data will be made available on request.

References

Al-Tahir R., Ali A.

Assessing land cover changes in the coastal zone using aerial photography

Surv. Land Inf. Sci., 64 (2) (2004), pp. 107-112

Alesheikh A.A., Ghorbanali A., Nouri N.

Coastline change detection using remote sensing

Int. J. Environ. Sci. Technol., 4 (1) (2007), pp. 61-66

Arkema K.K., Guannel G., Verutes G., Wood S.A., Guerry A., Ruckelshaus M., Kareiva P., Lacayo M., Silver J.M.

Coastal habitats shield people and property from sea-level rise and storms

Nature Clim. Change, 3 (10) (2013), pp. 913-918

Arpe K., Bengtsson L., Golitsyn G.S., Mokhov I.I., Semenov V.A., Sporyshev P.V.

Connection between Caspian Sea level variability and ENSO

Geophys. Res. Lett., 27 (17) (2000), pp. 2693-2696

Arpe K., Leroy S.A.G., Lahijani H., Khan V.

Impact of the European Russia drought in 2010 on the Caspian Sea level

Hydrol. Earth Syst. Sci., 16 (1) (2012), pp. 19-27

Arpe K., Molavi-Arabshahi M., Leroy S.A.G.

Wind variability over the Caspian Sea, its impact on Caspian seawater level and link with ENSO

Int. J. Climatol., 40 (14) (2020), pp. 6039-6054

Arpe K., Tsuang B.J., Tseng Y.H., Liu X.Y., Leroy S.A.

Quantification of climatic feedbacks on the Caspian Sea level variability and impacts from the Caspian Sea on the large-scale atmospheric circulation

Theor. Appl. Climatol., 136 (1) (2019), pp. 475-488, 10.1007/s00704-018-2481-x

Bagli, S., Soille, P., 2003. Morphological automatic extraction of Pan-European coastline from Landsat ETM+ images. In: Proceedings of the Fifth International Symposium on GIS and Computer Cartography for Coastal Zone Management, 2003. Genova.

Baig M.H.A., Zhang L., Shuai T., Tong Q.

Derivation of a Tasseled Cap transformation based on Landsat 8 at-satellite reflectance

Remote Sens. Lett., 5 (5) (2014), pp. 423-431

Bayram B., Acar U., Seker D., Ari A.

A novel algorithm for coastline fitting through a case study over the Bosphorus

J. Coast. Res., 24 (4) (2008), pp. 983-991

Bernstein L.S., Jin X., Gregor B., Adler-Golden S.M.

The quick atmospheric correction (QUAC) code: Algorithm description and recent upgrades

SPIE Opt. Eng., 51 (11) (2012), Article 111719

Crist E.P.

A TM Tasseled Cap equivalent transformation for reflectance factor data

Remote Sens. Environ., 17 (3) (1985), pp. 301-306

Crowell M., Leatherman S.P., Buckley M.K.

Historical shoreline change-error analysis and mapping accuracy

J. Coast. Res., 7 (1991), pp. 839-852

Dolan R., Michael S.F., Holme S.J.

Temporal analysis of shoreline recession and accretion

J. Coast. Res., 7 (3) (1991), pp. 723-744

Dolotov Y., Kaplin P.

Black and caspian seas, coastal ecology and geomorphology

Encyclopedia of Coastal Science, Springer (2005), pp. 194-203

Duck R.W., Figueiredo da Silva J.

Coastal lagoons and their evolution: a hydromorphological perspective

Estuar. Coast. Shelf Sci., 110 (2012), p. 2e14, 10.1016/j.ecss.2012.03.007

Ekercin S.

Coastline change assessment at the Aegean Sea coasts in Turkey using multitemporal Landsat imagery

J. Coast. Res., 23 (3) (2007), pp. 691-698

El-Asmar H.M., Hereher M.E., El Kafrawy S.B.

Surface area change detection of the Burullus Lagoon, North of the Nile Delta, Egypt, using water indices: a remote sensing approach

Egypt. J. Remote Sens. Space Sci., 16 (2013), pp. 119-123, 10.1016/j.ejrs.2013.04.004

Farley Nicholls J., Toumi R.

On the lake effects of the Caspian Sea

Q. J. R. Meteorol. Soc., 140 (681) (2014), pp. 1399-1408

Feyisa G.L., Meilby H., Fensholt R., Proud S.R.

Automated water extraction index: a new technique for surface water mapping using landsat imagery

Remote Sens. Environ., 40 (2014), pp. 23-35, 10.1016/j.rse.2013.08.029

Fisher A., Flood N., Danaher T.

Comparing landsat water index methods for automated water classification in eastern Australia

Remote Sens. Environ., 175 (2016), pp. 167-182, 10.1016/j.rse.2015.12.055

Ford F.

Shoreline changes interpreted from multi-temporal aerial photographs and high resolution satellite images: Wotje Atoll, Marshall Islands

Remote Sens. Environ., 135 (2013), pp. 130-140, 10.1016/j.rse.2013.03.027

García-Rubio G., Huntley D., Russell P.

Evaluating shoreline identification using optical satellite images

Mar. Geol., 359 (2015), pp. 96-105

Genz A.S., Fletcher C.H., Dunn R.A., Frazer L.N., Rooney J.J.

The predictive accuracy of shoreline change rate methods and alongshore beach variation on Maui, Hawaii

J. Coast. Res., 23 (1) (2007), pp. 87-105

Ghanavati E., Firouzabadi P.Z., Jangi A.A., Khosravi S.

Monitoring geomorphologic changes using Landsat TM and ETM+ data in the Hendijan River delta, south west Iran

Int. J. Remote Sens., 29 (4) (2008), pp. 945-959

Haghani S., Leroy S.A., Wesselingh F.P., Rose N.L.

Rapid evolution of coastal lagoons in response to human interference under rapid sea level change: A south Caspian Sea case study

Quat. Int., 408 (2016), pp. 93-112

Hamzeh, S., Akbari, E., Kakroodi, A.A., Jeihooni, M., 2017. Investigation the dynamic response of the Anzali lagoon to sea-level changes using multi-sources remotely sensed data. In: The 38th Asian Conference on Remote Sensing. New Delhi, pp. 23–27.

Huang C., Wylie B., Yang L., Homer C., Zylstra G.

Derivation of a Tasseled Cap transformation based on Landsat 7 at-satellite reflectance

Int. J. Remote Sens., 23 (8) (2002), pp. 1741-1748

Jain S.K., Singh R.D., Jain M.K., Lohani A.K.

Delineation of flood-prone areas using remote sensing techniques

Water Resour. Manag., 19 (2005), pp. 333-347

Jeihouni M., Kakroodi A.A., Hamzeh S.

Monitoring shallow coastal environment using Landsat/altimetry data under rapid sea-level change

Estuar. Coast. Shelf Sci., 224 (2019), pp. 260-271

Kakroodi A.A., Kroonenberg S.B., Goorabi A., Yamani M.

Shoreline response to rapid 20th century sea-level change along the Iranian Caspian coast

J. Coast. Res., 30 (6) (2014), pp. 1243-1250

Kakroodi A.A., Kroonenberg S.B., Hoogendoorn R.M., Mohammadkhani H., Yamani M., Ghasssemi M.R., Lahijani H.A.K.

Rapid Holocene sea-level changes along the Iranian Caspian coast

Quat. Int., 263 (93H.A) (2012)

Kakroodi A.A., Kroonenberg S.B., Naderi Beni A., Noehgar N.

Short- and long-term development of the Miankaleh Spit, Southeast Caspian Sea

Iran. J. Coast. Res., 30 (6) (2014), pp. 1236-1242

Kakroodi A.A., Leroy S.A.G., Kroonenberg S.B., Lahijani H.A.K., Alimohammadian H., Boomer I., Goorabi A.

Late pleistocene and Holocene sea-level change and coastal paleoenvironment evolution along the Iranian Caspian shore

Mar. Geol., 361 (2015), pp. 111-125

Kaplin P.A., Selivanov A.O.

Recent coastal evolution of the Caspian Sea as a natural model for coastal responses to the possible acceleration of global sea level rise

Mar. Geol., 124 (1) (1995), pp. 161-175

Kauth R., Lambeck P., Richardson W., Thomas G., Pentland A.

Feature extraction applied to agricultural crops as seen by landsat

Proceedings of the LACIE Symposium, Houston TX, NASA (1979), pp. 705-721

Kauth R.J., Thomas G.S.

The tasseled cap – a graphic description of the spectral–temporal development of agricultural crops as seen in Landsat

Proceedings on the Symposium on Machine Processing of Remotely Sensed Data, West Lafayette, Indiana, June 29 – July 1, 1976, LARS, Purdue University, West Lafayette, Indiana (1976), pp. 41-51

Kermani S., Boutiba M., Guendouz M., Guettouche M.S., Khelfani D.

Detection and analysis of shoreline changes using geospatial tools and automatic computation: Case of jijelian sandy coast (East Algeria)

Ocean Coast. Manag., 132 (2016), pp. 46-58

Kirwan M.L., Megonigal J.P.

Tidal wetland stability in the face of human impacts and sea-level rise

Nature, 504 (2013), pp. 53-60

Klein I., Dietz A.J., Gessner U., Galayeva A., Myrzakhmetov A., Kuenzer C.

Evaluation of seasonal water body extents in Central Asia over the past 27 years derived from medium-resolution remote sensing data

Int. J. Appl. Earth Obs. Geoinf., 26 (2014), pp. 335-349

Koriche S.A., Singarayer J.S., Cloke H.L., Valdes P.J., Wesselingh F.P., Kroonenberg S.B., Wickert A.D., Yanina T.A.

What are the drivers of Caspian Sea level variation during the late Quaternary?

Quat. Sci. Rev., 283 (2022), Article 107457

Kosarev A.N.

Physicoegeographical conditions of the Caspian Sea

Kostianoy A., Kosarev A. (Eds.), The Caspian Sea Environment, Springer (2005), pp. 5-31

Kroonenberg S.B., Abdurakhmanov G.M., Badyukova E.N., Borg K.V.D., Kalashnikov A., Kasimov N.S., Rychagov G.I., Svitoch A.A., Vonhof H.B., Wesselingh F.P.

Solareforced 2600 BP and little Ice Age highstands of the Caspian Sea

Quat. Int., 173 (2007), pp. 137-143

Kuleli T.

Change detection and assessment using multi temporal satellite image for North-East Mediterranean Coast

GIS Dev. Weekly, 1 (5) (2005)

Kuleli T.

Quantitative analysis of shoreline changes at the Mediterranean Coast in Turkey

Environ. Monit. Assess., 167 (1–4) (2009), pp. 387-397

Kuleli T., Guneroglu A., Karsli F., Dihkan M.

Automatic detection of shoreline change on coastal Ramsar wetlands of Turkey

Ocean Eng., 38 (10) (2011), pp. 1141-1149

Leroy S.A.G., Lahijani H.A.K., Djamali M., Naqinezhad A., Moghadam M.V., Arpe K., Shah-Hosseini M., Hosseindoust M., Miller Ch.S., Tavakoli V., Habibi P., Naderi Beni M.

Late Little Ice Age palaeoenvironmental records from the Anzali and Amirkola Lagoons (south Caspian Sea): Vegetation and sea level changes

Palaeogeogr. Palaeoclimatol. Palaeoecol., 302 (2011), pp. 415-434,

Li W., Gong P.

Continuous monitoring of coastline dynamics in western Florida with a 30-year time series of Landsat imagery

Remote Sens. Environ., 179 (2016), pp. 196-209

Lira J.

Segmentation and morphology of open water bodies from multispectral images

Int. J. Remote Sens., 27 (2006), pp. 4015-4038

Liu Y., Huang H., Qiu Z., Fan J.

Detecting coastline change from satellite images based on beach slope estimation in a tidal flat

Int. J. Appl. Earth Obs. Geoinf., 23 (2013), pp. 165-176

Maiti S., Bhattacharya A.K.

Shoreline change analysis and its application to prediction: a remote sensing and statistics based approach

Mar. Geol., 257 (1–4) (2009), pp. 11-23

Manca E., Pascucci V., Deluca M., Cossu A., Andreucci S.

Shoreline evolution related to coastal development of a managed beach in Alghero, Sardinia, Italy

Ocean. Coast. Manag., 85 (2013), pp. 65-76, 10.1016/j.ocecoaman.2013.09.008

Marfai M.A., Almohammad H., Dey S., Susanto B., King L.

Coastal dynamic and shoreline mapping: multi-sources spatial data analysis in Semarang Indonesia

Environ. Monitor. Assess., 142 (2008), pp. 297-308

McFeeters S.K.

The use of the normalized difference water index (NDWI) in the delineation of open water features

Int. J. Remote Sens., 17 (1996), pp. 1425-1432, 10.1080/01431169608948714

Mills J.P., Buckley S.J., Mitchell H.L., Clarke P.J., Edwards J.

A geomatics data integration technique for coastal change monitoring

Earth Surface Process. Landforms, 30 (6) (2005), pp. 651-664

Moser, L., Voigt, S., Schoepfer, E., 2014. Monitoring of critical water and vegetation anomalies of Sub-Saharan West-African wetlands. In: Proceedings of the IEEE International Conference on Geoscience and Remote Sensing Symposium. Québec City, QC, Canada, pp. 3842–3845.

Moussaid J., Fora A.A., Zourarah B., Maanan M., Maanan M.

Using automatic computation to analyze the rate of shoreline change on the Kenitra coast, Morocco

Ocean Eng., 102 (2015), pp. 71-77

Naderi Beni A., Lahijani H.A.K., Harami R.M., Arpe K., Leroy S.A.G., Marriner N., Berberian M., AndrieuePonel V., Djamali M., Mahboubi A.

Caspian sea level changes during the last millennium: historical and geological evidences from the south Caspian Sea

Climate Past, 9 (2013), pp. 1645-1665

NASA

Landsat 7 science data users handbook, (on-line)

(2006)

available on. http://landsathandbook.gsfc.nasa.gov/pdfs/Landsat7_Handbook.pdf (December, 2016)

Natesan U., Parthasarathy A., Vishnunath R., Kumar G.E.J., Ferrer V.A.

Monitoring long term shoreline changes along Tamil Nadu, India using geospatial techniques

Aquat. Proc., 4 (2015), pp. 325-332, 10.1016/j.aqpro.2015.02.044

Nicholls R.J., Cazenave A.

Sea-level rise and its impact on coastal zones

Science, 328 (2010), pp. 1517-1520

Ouma Y.O., Tateishi R.

A water index for rapid mapping of shoreline changes of five East African Rift Valley lakes: An empirical analysis using Landsat TM and ETM+ data

Int. J. Remote Sens., 27 (2006), pp. 3153-3181

Ozturk D., Sesli F.A.

Shoreline Change Analysis of the Kizilirmak Lagoon Series Ocean & Coastal Management

(2015), pp. 1-19, 10.1016/j.ocecoaman.2015.03.009

In press

Pardo-Pascual J.E., Almonacid-Caballer J., Ruiz L.A., Palomar-Vázquez J.

Automatic extraction of shorelines from Landsat TM and ETM+ multi-temporal images with subpixel precision

Remote Sens. Environ., 123 (2012), pp. 1-11

Rebelo L.M., Finlayson C.M., Nagabhatla N.

Remote sensing and GIS for wetland inventory, mapping and change analysis

J. Environ. Manag., 90 (2009), pp. 2144-2153

Scott J.W., Moore L.R., Harris W.M., Reed M.D.

Using the landsat 7 enhanced thematic mapper tasseled cap transformation to extract shoreline

(2003)

Sesli F.A., Karsli F., Colkesen I., Akyol N.

Monitoring the changing position of coastlines using aerial and satellite image data: an example from the eastern coast of Trabzon, Turkey

Environ. Monit. Assess., 153 (1–4) (2008), pp. 391-403

Shaghude Y.W., Wannäs K.O., Lundeń B.

Assessment of shoreline changes in the western side of Zanzibar channel using satellite remote sensing

Int. J. Remote Sens., 24 (23) (2003), pp. 4953-4967

Singh A.

Digital change detection techniques using remotely sensed data

Int. J. Remote Sens., 10 (1989), pp. 989-1003

Soliman G., Soussa H.

Wetland change detection in Nile swamps of southern Sudan using multi temporal satellite imagery

J. Appl. Remote Sens., 5 (2011), Article 053517, 10.1117/1.3571009

Thieler, E.R., Himmelstoss, E.A., Zichchi, J.L., Miller, T.L., 2005. Digital Shorline Analysis System (DSAS) Version Version 3.0: an Arc GIS Extension for Calculating Shorline Change. US. Geological survey. Open-file Report 2005-1304.

USDA (2016)

https://www.pecad.fas.usda.gov/cropexplorer/global_reservoir (last accessed 12.30.16)

Van T.T., Binh T.T.

Application of remote sensing for shoreline change detection in Cuu Long Estuary

VNU J. Sci. Earth Sci., 25 (2009), pp. 217-222

Vanderstraete T., Goossens R., Ghabour T.K.

The use of multi-temporal landsat images for the change detection of the coastal zone near Hurghada, Egypt

Int. J. Remote Sens., 27 (17) (2006), pp. 3645-3655

Webb E.L., Friess D.A., Krauss K.W., Cahoon D.R., Guntenspergen G.R., Phelps J.

A global standard for monitoring coastal wetland vulnerability to accelerated sea-level rise

Nature Clim. Change, 3 (2013), pp. 458-465

Wu W.

Coastline evolution monitoring and estimation—a case study in the region of Nouakchott, Mauritania

Int. J. Remote Sens., 28 (24) (2007), pp. 5461-5484

Xu H.

Modification of normalized difference water index (NDWI) to enhance open water features in remotely sensed imagery

Int. J. Remote Sens., 27 (2006), pp. 3025-3033

Yang X., Damen M.C.J., Van Zuidam R.A.

Use of Thematic Mapper imagery with a geographic information system for geomorphologic mapping in a large deltaic lowland environment

Int. J. Remote Sens., 20 (4) (1999), pp. 659-681

Yang J., Gong P., Fu R., Zhang M., Chen J., Liang S., Xu B., Shi J., Dickinson R.

The role of satellite remote sensing in climate change studies

Nature Clim. Change, 3 (10) (2013), pp. 875-883